Cardiac Troponin T Forms a Tetramer in Vitro†

Karim C. Lounes,‡,§ Borries Demeler,|| David E. Anderson,⊥ Aldrin W. Gomes,@ James D. Potter,# Rashid Nassar,‡ and Page A. W. Anderson*,‡

Department of Pediatrics, Duke University Medical Center, Durham, North Carolina 27710, Department of Biochemistry, University of Texas Health Science Center, San Antonio, Texas 78229, Department of Cell Biology, Duke University Medical Center, Durham, North Carolina 27710, Department of Physiology, University of California, Los Angeles, California 90095, and Department of Molecular and Cellular Pharmacology, University of Miami, Miami, Florida 33124

Received June 27, 2007; Revised Manuscript Received December 6, 2007

ABSTRACT: Cardiac troponin T (cTnT) is a myofibrillar protein essential for calcium-dependent contraction. This property has led to functional studies of developmentally expressed cTnT isoforms and mutants identified in patients with hypertrophic cardiomyopathy. The release of cTnT into the serum following myocardial infarction has led to the development of antibody-based assays for measuring cTnT serum concentration. We examined the behavior of cTnT in solution. Recombinant human $cTnT_3$, the dominant isoform in the adult human heart, was used. The protein was pure and functional, as demonstrated by SDS−PAGE and surface plasmon resonance. $cTnT_3$ was found to bind specifically and in a concentration-dependent manner to cTnC. Routine size exclusion chromatography suggested a higher-than-expected MW for cTnT. Using analytical ultracentrifugation, we found $cTnT_3$ in solution to be mainly in the form of a tightly bound tetramer at concentrations as low as 4 μmol/L. Our sedimentation velocity and transmission electron microscopy results indicate that the tetramer's shape is elongated rather than globular. CTnT's self-association in solution is an important consideration in the design and interpretation of experiments with the aim of understanding the biochemical and biophysical properties of cTnT, its isoforms, and its mutants.

Troponin regulates striated muscle contraction. Troponin is made up of three subunits, troponin C (TnC), TnI, and TnT in a stoichiometry of 1:1:1. TnT binds troponin to tropomyosin and is essential for calcium-regulated contraction (*1*). Cardiac TnT isoforms and cTnT[1] mutants, expressed in patients with hypertrophic cardiomyopathy or in solution or overexpressed in the cell by adenovirus vectors, have been used to replace cTnT in cardiac myofilaments to test their functional consequences (*2*−*9*). Cardiac TnT is known to circulate as a free intact form in patients (*10*), and certain diseases may increase the amount of free cTnT in the blood (*10*, *11*). Antibody-based assays are used to measure serum cTnT concentration. Self-association of cTnT in solution could affect the design and interpretation of replacement experiments and could be relevant to the design of clinical assays.

The inherent binding properties of cTnT in solution are not known. Studies of cTnT structure have been limited due to its poor solubility and apparent tendency to aggregate (*12*, *13*). In this study, we used ultracentrifugation techniques and transmission electron microscopy to examine in a rigorous manner the properties of purified recombinant human cTnT in solution. We found that in solution cTnT was mainly in the form of a tightly bound tetramer.

MATERIALS AND METHODS

Proteins. cTnT and cTnC proteins were expressed in *Escherichia coli*, purified as previously described (*3*), and stored in urea. To prevent carbamylation, (a) all charged particles that may be present in the urea were first removed using a mixed bead resin [AG501-X8 (D), Bio-Rad], (b) all procedures were carried out at 4−6 °C in a cold room, (c) the pH was always adjusted to 6.5 for storage in 6 mol/L urea to prevent carbamylation, (d) carbamylation was also prevented via storage at −80 °C, and (e) once cTnT was removed from the freezer, it was dialyzed into the desired buffer in a cold room. The proteins were refolded in vitro before use (*8*), using a series of dialysis steps. The first buffer consisted of 0.02 mol/L MOPS, 3.0 mol/L urea, 1.0 mol/L KCl, and 0.001 mol/L DTT (pH 7.2). The urea concentration was reduced stepwise to 1 mol/L and then removed, followed by reduction of the KCl concentration to 0.7 and 0.5 mol/L. The preparations were spun at 60000*g* (30 min) to remove aggregates, concentrated using centrifugal concentrators (10 kDa cutoff, Amicon, Inc., and examined using SDS−PAGE and Western blot analysis (*14*, *15*).

† Supported in the part by NHLBI Grant HL42250 (P.A.W.A.), NIH Grant HL42325 (J.D.P.), NIH Grant HL674154 (J.D.P.), NHLBI Grant HL67385 (B.D.), and NIH Grant 1R01RR022200 (B.D.)

* To whom correspondence should be addressed: Pediatric Cardiology, Duke University Medical Center, Research Park Bldg. II, Room 113, Box 3218, Durham, NC 27710. Phone: (919) 684-6027. Fax: (919) 684-4609. E-mail: ander005@mc.duke.edu.

‡ Department of Pediatrics, Duke University Medical Center.

§ Present address: Biolex, Inc., Pittsboro, NC 27312.

|| University of Texas Health Science Center.

⊥ Department of Cell Biology, Duke University Medical Center.

@ University of California.

University of Miami.

[1] Abbreviations: SPR, surface plasmon resonance; cTnT, cardiac troponin T; cTnI, cardiac troponin I; cTnC, cardiac troponin C; OD, optical density; MW, molecular weight.

10.1021/bi7012596 CCC: $40.75
Published on Web 01/16/2008

Surface Plasmon Resonance. Binding of $cTnT_3$ to cTnC was performed using a Biacore 3000 instrument (Biacore Inc.). cTnC was immobilized on a CM5 sensor chip (Biacore, Inc.) using the amine coupling kit, as recommended by the manufacturer. After the chip had been activated, a cTnC solution [20 μg/mL, 10 mmol/L sodium acetate (pH 4.0)] was applied at 5 μL/min until the desired amount of protein was immobilized (300−800 resonance units). The sensor chip was then deactivated. A control flow cell without protein was treated similarly. $cTnT_3$, at different concentrations in running buffer [0.3 mol/L KCl and 0.02 mol/L MOPS (pH 7.2)], was used at a rate of 15 μL/min for 2 min. After each injection, the flow cells were regenerated by injecting MOPS-buffered solution containing 1 mol/L KCl at 30 μL/min for 3 min.

Analytical Ultracentrifugation. Sedimentation velocity and sedimentation equilibrium experiments were used to study $cTnT_3$ oligomerization properties. Sedimentation experiments were performed with a Beckman Optima XL-A instrument. Data analysis was performed with UltraScan version 9.3 (http://www.ultrascan.uthscsa.edu/). Hydrodynamic corrections for buffer conditions were made with UltraScan according to data published by Laue et al. (*16*). The partial specific volume of $cTnT_3$, estimated from its known peptide sequence according to the method of Durchschlag (*17*), was estimated to be 0.712 cm^3/g. All the samples were analyzed at 4 °C in a buffer containing 0.02 mol/L potassium phosphate or MOPS and 0.5 mol/L KCl (pH 7.2). Sedimentation scans were collected at equilibrium at 275 nm and at 230 nm in radial step mode with a 0.001 cm step size and 20-point averages. Multiple loading concentrations between 0.3 and 0.7 OD were used; data for which OD > 0.9 were excluded. Equilibrium data in the concentration range between 1 and 40 μmol/L were examined. For reversibly self-associating models, we converted absorbance measurements into molar concentrations to obtain the fit for a global equilibrium constant. The extinction coefficient at each wavelength was taken into account. Extinction coefficients at 220, 230, 275, and 280 nm were determined by the global fitting of absorbance wavelength scans as described by Demeler (*18*) and found to be 163370, 84030, 17420, and 16500 mol^{-1} cm^{-1}, respectively. Sedimentation velocity experiments were conducted at 50000 rpm and measured at 220, 230, and 280 nm. Loadings at these wavelengths corresponded to concentrations of 2, 4, 14, and 40 μmol/L. van Holde−Weischet analysis (*19*) was used to determine sedimentation coefficient distributions and to derive models for whole boundary fitting. Whole boundary fits were performed with the ASTFEM solution of the Lamm equation (*20*), using the optimization method described by Demeler and Saber (*21*). Statistics were evaluated using the Monte Carlo procedure implemented in UltraScan.

Transmission Electron Microscopy. (i) Glycerol Gradient Sedimentation. Samples were centrifuged through a 5 mL, 15 to 40% glycerol gradient in 0.2 mol/L NH_4HCO_3, to estimate sedimentation coefficients, and transferred into an appropriate buffer for rotary shadowing. After sedimentation at 38000 rpm and 20 °C for 16 h on the SW55.1 rotor (Beckman Instruments), gradient fractions were collected and analyzed by SDS−PAGE. Sedimentation coefficients were determined by linear interpolation of standard curves (*22*) constructed using proteins of known sedimentation coefficients, included in the same centrifugation run.

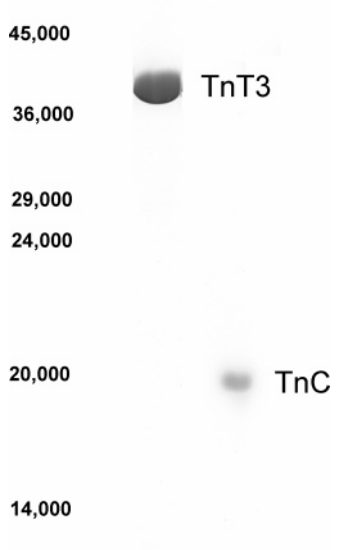

FIGURE 1: SDS−PAGE of $cTnT_3$ and cTnC. The standard MW markers (daltons) are indicated on the left side of the gel.

(ii) Rotary Shadowing and Electron Microscopy. The peak fraction, corresponding to a sedimentation coefficient of ~5 S, was diluted in 0.2 mol/L NH_4HCO_3 (pH 8.2) containing 30% glycerol to a final concentration of ~50 μg/mL and rotary shadowed, as described previously (*23*). Specimens were viewed under a transmission electron microscope (model 301, Philips Electron Optics), and photographs were taken at a magnification of 50000×. Negatives were scanned at 600 dpi, using an Epson 4870 Photo scanner, and imported into NIH Image or ImageJ for measurement and analysis.

RESULTS

Structural and Functional Integrity of $cTnT_3$. $cTnT_3$ purity was verified (Figure 1). Coomassie-stained SDS−PAGE gels showed a single band. $cTnT_3$ migrated at a molecular weight (MW) of 39 kDa, the same as the electrophoretic mobility of $cTnT_3$ in human myocardium never exposed to urea (*24*). The same higher-than-expected MW on SDS−PAGE has been seen in cTnT in rat myocardial samples that have never been exposed to urea (*25*). This higher-than-expected MW may reflect cTnT having a highly acidic N-terminal region which has been suggested to alter the binding of negatively charged SDS. Western blots, using a cTnT-specific monoclonal antibody (*26*), demonstrated a single band (results not shown).

Routine size exclusion chromatography analysis indicated $cTnT_3$ may form higher-MW molecules in solution. A 1 mg/mL solution in 20 mmol/L MOPS and 0.5 mol/L KCl (pH 7.2) was analyzed on a Sephacryl S200 column (Amersham Biosciences). The protein eluted as a single peak (close to the void volume of the column) corresponding to a protein having a MW much higher than 34.5 kDa (data not shown).

The functional properties of $cTnT_3$ were examined using surface plasmon resonance (Figure 2). Binding kinetic profiles of different $cTnT_3$ concentrations are illustrated in Figure 2A. To remain consistent with the previously published data, a dissociation constant was derived assuming the model of one molecule of cTnT binding one molecule

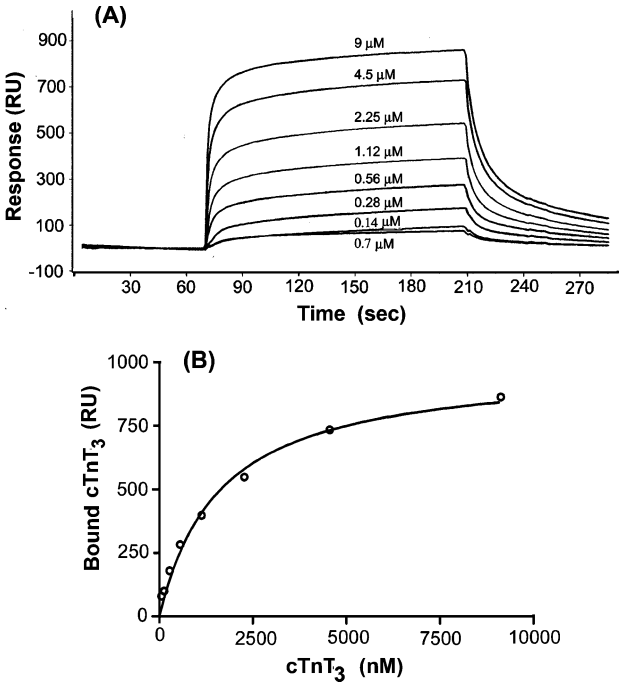

FIGURE 2: $cTnT_3$ binding to immobilized cTnC measured by SPR. (A) Kinetic binding profiles of the indicated concentrations of $cTnT_3$ to immobilized cTnC. Nonspecific binding to the control flow cell was subtracted. (B) Bound $cTnT_3$ as a function of cTnT concentration. The line is the fit to the single-binding site model, yielding a K_d of 119 nmol. The bound $cTnT_3$ (Y) was plotted as a function of cTnT concentration ([$cTnT_3$]) and fitted to the equation $Y = (B_{max}\text{-}[cTnT_3])/(K_d + [cTnT_3])$. For each $cTnT_3$ concentration, Y corresponds to the signal in resonance units at the highest point of the corresponding SPR trace. The parameters K_d and B_{max} were derived from the fit.

of TnC. Furthermore, the molecule of cTnT was assumed to be a monomer, and its molar concentration was calculated accordingly. Details of the fit of the binding data are provided in the legend of Figure 2. This analysis yielded a dissociation constant of 1.2 μmol/L, close to values reported previously for the skeletal muscle TnT−TnC species (*27*). These results indicated that our $cTnT_3$ preparations migrated as a single band and were virtually free of any contaminant. SPR data suggest that $cTnT_3$ binds to immobilized cTnC in a concentration-dependent manner.

Analytical Ultracentrifugation Analysis (AUC). Velocity analysis reveals information about the presence of aggregates and about the composition of the sample. For reversibly self-associating systems, global equilibrium analysis can determine the molecular weights and equilibrium constants of the components present in the system. The molecular weight of the monomer and the K_d are considered global parameters and forced to be the same for all included data sets (*28*). The composition of $cTnT_3$ at four loading concentrations (from 2 to 40 μmol/L) was characterized using sedimentation velocity measurements. van Holde−Weischet analysis of the data suggested a single-ideal species model for all the protein concentrations except the two lowest (2 and 4 μmol/L at 220 nm), where evidence of additional slower-sedimenting species was present (Figure 3).

Samples for which the van Holde−Weischet analysis indicated a single ideal species (*20*) were fit to a single-ideal species model using the whole boundary method (*21*); the fit indicated a molecular mass ~4 times greater than that

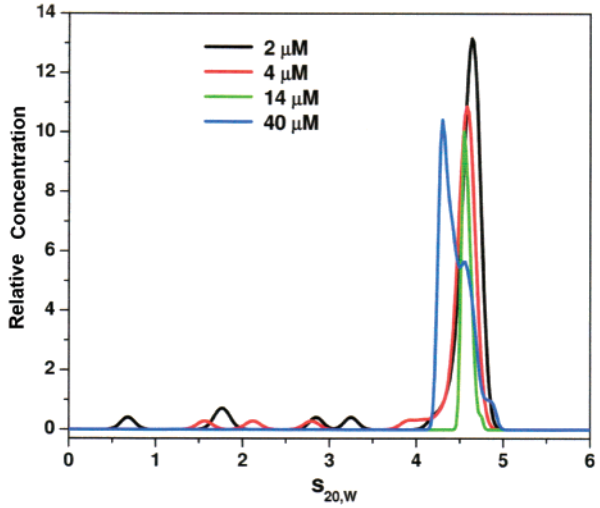

FIGURE 3: Sedimentation velocity. van Holde−Weischet $s_{20,W}$ distributions for four samples of $cTnT_3$ at 2, 4, 14, and 40 μmol/L. The highest concentration displays a noticeable decrease in the sedimentation coefficient due to concentration-dependent nonideality. The two lowest concentrations show a lower-molecular weight species, presumably from dissociation into a dimer. All other concentrations display a homogeneous sedimentation coefficient distribution. The large sedimentation coefficient peak at 4.6 S corresponds to a tetrameric species.

predicted for the monomer molecular weight of $cTnT_4$ of 34.6 kDa, suggesting that the protein exists as a tetramer under the conditions of the test. To test the extent of dissociation of the tetramer into smaller oligomers, we used a concentration of 14 μmol/L to fit a two-species model, which indicated that 92.8% of the protein exists as a tetramer and 7.2% as a dimer. Even though the two-component fit resulted in a second species with a molecular weight consistent with the dimer, not enough signal was available to make a reliable determination of shape. Consequently, the frictional ratio of 1.1 may be an underestimate. The results are summarized in Table 1.

The sedimentation coefficients estimated from both methods agreed well. A slight decrease in the sedimentation coefficient with an increasing concentration was detected in both, likely due to concentration-dependent nonideality of $cTnT_3$. The highest concentration examined (40 μmol/L) exhibited appreciable concentration-dependent nonideality effects as judged by the van Holde−Weischet integral distribution plot (data not shown and ref *29*), causing a reduction in the sedimentation coefficient which was evident in the blue curve of Figure 3 by showing a slightly reduced s value with only a shoulder where the lower concentrations peaked. We ascribe this nonideality to the elongated shape and relatively large frictional ratio observed in the finite element fit (below). The whole boundary fit resulted in a molecular weight (Table 1) that was in excellent agreement with a tetrameric oligomerization state of $cTnT_3$. From the whole boundary fit, we characterized the overall shape of the tetrameric form of $cTnT_3$. The derived frictional ratios (f/f_0) ranged from 2.16 to 2.34, indicating that oligomerized $cTnT_3$ molecules in solution have an elongated shape.

To examine further the oligomerization state of $cTnT_3$ and the association constant for the dimer−tetramer equilibrium, we performed equilibrium analysis over a broad range of concentrations (from 0.7 to 22 μmol/L) at 230 and 280 nm. We modeled the dimer−tetramer equilibrium of cTnT by

Table 1: $cTnT_3$ Sedimentation Equilibrium and Velocity Results[a]

method	molecular weight (kDa)	dissociation constant (K_d)	sedimentation coefficient $s_{20,w}$ (S)	frictional ratio f/f_0
equilibrium, single-ideal species model	137.1 (136.3−138.3)	−	−	−
equilibrium, dimer−tetramer model	69.56 (67.99−71.92)	127 nM (33−717 nM)	−	−
velocity, whole boundary fit (4 μmol/L) (one-species fit)	134.8	−	4.60	2.16
velocity, whole boundary fit (14 μmol/L) (two-species fit)	tetramer	144.6 (9.8%)	4.62	2.25
	dimer	78.3 (7.2%)	6.28	1.10
velocity, whole boundary fit (40 μmol/L) (one-species fit)	149.3	−	4.55	2.34

[a] Values in parentheses are 95% confidence intervals determined by Monte Carlo analysis. The concentration-dependent nonideality at the high concentration measurement (40 μmol/L) results in an artificial sharpening of the boundary that may result in underestimation of the diffusion coefficient and, hence, overestimation of the molecular weight. All molecular weight values agree well with either the tetramer or dimer of $cTnT_3$. The K_d (dimer−tetramer) obtained from the two-species model was 127 nmol/L; the large 95% confidence interval (33−717 nmol/L) suggests that little signal was available for fitting this parameter, while sufficient signal was present to estimate the dimer molecular weight reliably.

both a single-ideal species model and a reversibly self-associating monomer−dimer model. The single-species model fit (residual variance of 3.8133×10^{-5} cm^{-2}) gave a MW of 137.1 kDa, corresponding to the tetramer, whereas the two-species model fit (residual variance of 3.8065×10^{-5} cm^{-2}**)** gave a MW of 69.6 kDa and a K_d for tetramer−dimer dissociation of 127 nmol/L. The residual variance differed little between the two models, indicating that the two-species model did not fit the data significantly better than the single-species model and that very little dimer signal was present in the data, making the uncertainty in the determination of the tetramer−dimer K_d large.

Figure 4A shows a global, single-species fit of equilibrium scans acquired from two independently folded $cTnT_3$ protein samples at concentrations ranging from 2 to 40 μmol/L, at two speeds and two wavelengths. The molecular weight determined by the single-ideal species model is in excellent agreement with the molecular weight of a tetrameric $cTnT_3$ oligomer, with an expected molecular weight of 137.8 kDa calculated from the sequence. The fit to the two-species model resulted in a molecular weight in good agreement with the dimer oligomeric species, suggesting a reversible equilibrium between the dimer and tetramer with a low K_d. To assess the accuracy of the estimated K_d, Monte Carlo analysis was performed on the two-species dimer−tetramer fit. It showed a broad 95% confidence interval for the K_d that is likely due to the small amount of protein existing as a dimer. A plot of the equilibrium isotherms for dimer and tetramer, as well as the relative signal observed in the experiment, is shown in Figure 4B. As one can see from the plot, only ~20% of the dimer concentration is observed at the lowest measurable concentration in this experiment, which explains the relatively large 95% confidence intervals for the determined K_d. This limitation is imposed by the extinction properties of the protein and the sensitivity of the absorption optics in the analytical ultracentrifuge. We concluded that $cTnT_3$ in solution, under the described experimental conditions, tightly self-associates, mainly into tetramers.

Glycerol Gradient Sedimentation and Electron Microscopy. A solution of 1 mg/mL $cTnT_3$ was analyzed on a 15 to 40% glycerol gradient (see Materials and Methods). The protein sediments as a single peak with a sedimentation coefficient of 5 S (data not shown), in agreement with the analytical ultracentrifugation measurements. This fraction of $cTnT_3$ was prepared for transmission electron microscopy. Figure 5A shows a representative picture of the rotary-shadowed molecules. $cTnT_3$ appears as thin, rod-shaped molecules. Measurements of a sample of ~70 molecules are shown in Figure 5B. The median length of the molecule was 30 nm (range from 15 to 65 nm).

DISCUSSION

The central role of cTnT in calcium-dependent contraction has led to studies of cTnT and the biochemical and biophysical consequences of its isoforms and mutants. Our study's novel results demonstrate that cTnT tetramer formation in solution must be an important consideration of experiments in which these properties are being examined.

Studies of cTnT and cTnI mutants expressed in patients with hypertrophic cardiomyopathy have used displacement of cTnT from the myofilaments with cTnT in solution (*2*, *4*−*6*, *8*, *9*, *30*). The displacement of troponin from the myofilaments with mutant cTnT and adenovirus-induced expression of cTnT mutants have described different effects on myofilament calcium sensitivity of the same mutants (*6*−*8*). In skinned muscle fiber displacement experiments, micromolar concentrations of cTnT, where the dominant species is a cTnT tetramer, are used. Lower cTnT concentrations are not effective in displacing the native troponin complex. Successful displacement is evidenced by the fibers no longer being calcium-regulated. When a preformed TnI−TnC complex is added, the fibers become calcium-regulated. These findings support the likelihood that the cTnT tetramer binds the tropomyosin, in that SDS−PAGE of these fibers indicates a 1:1:1 cTnT:cTnI:cTnC stoichiometry (*31*). In some way, either the cTnT tetramer depolymerizes once cTnT binds to tropomyosin or the binding of the cTnI−cTnC complex causes disruption of the tetramer. These possibilities aside, the form of the troponin complex in the fiber is not known.

The expression of cTnT only in the heart in the adult and the release of cTnT in different forms from the myocardium, as troponin, cTnT−cTnI complex, cTnT, and fragments of cTnT, after myocardial infarction have led to the use of assays for measuring cTnT serum concentration to assess the presence of myocardial damage (*10*, *11*). The relevance of our finding of cTnT self-association to the use of these clinical assays is uncertain. Given that the concentrations measured in the patient are at the nanomolar level, the K_d for monomer−dimer association may be relevant. However, the limitations imposed by the extinction properties of the protein and the sensitivity of the absorption optics prevent us from knowing the form in which cTnT exists at low nanomolar concentrations.

Hydrodynamic studies of skeletal and cardiac troponin complexes have reported molecular weights much larger than

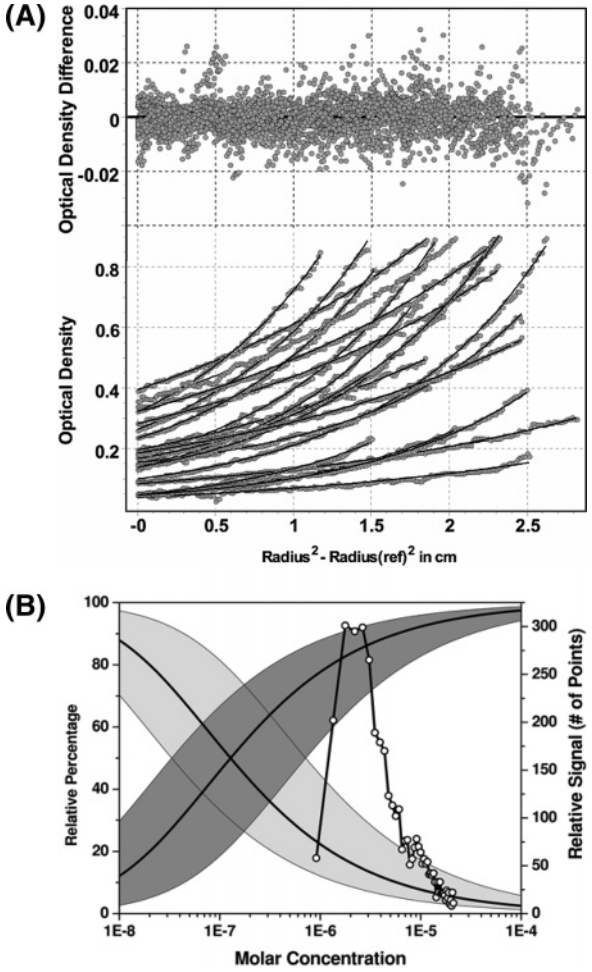

FIGURE 4: (A) Sedimentation equilibrium. Global equilibrium fit of cTnT3 to a single-ideal species model. Twenty sedimentation equilibrium data sets acquired at nine $cTnT_3$ concentrations ranging between 2 and 40 μmol/L and taken at two rotor speeds (7000 and 10000 rpm) are shown (gray circles). The solid lines represent the global fit of the data using the single-ideal species model (bottom panel). Residuals are shown in the top panel. (B) Shown here are the isotherms for the relative percentages of dimer and tetramer (solid black lines) at different molar concentrations. The light grey shaded area represents the 95% confidence intervals for the dimer, and the dark gray shaded area represents the 95% confidence intervals for the tetramer. The line with open circles indicates the relative signal strength in the global fitting experiment at different molar concentrations; it is a measure of the number of datapoints available for the global fit at different concentrations. As can be seen from the plot, only about 20% of dimer concentration is observed at the lowest measurable concentration in this experiment, which explains the relatively large 95% confidence intervals for the determined K_d.

those expected from the normal stoichiometry of the troponin subunits of 1:1:1 (*32*, *33*). cTnC is known to be monomeric in solution (*34*), and cTnI has been found to be essentially monomeric at concentrations near 1 mg/mL (*35*). cTnT self-association can explain the higher-than-expected MW of troponin in solution.

Our results provide strong evidence that in solution, $cTnT_3$, the dominantly expressed isoform in the adult human heart (*36*), self-associates tightly to form a tetramer. The molecular weights derived from velocity and equilibrium sedimentation experiments agree well with the expected MW for either dimer or tetramer when calculated from the peptide sequence. Furthermore, van Holde−Weischet analysis demonstrated

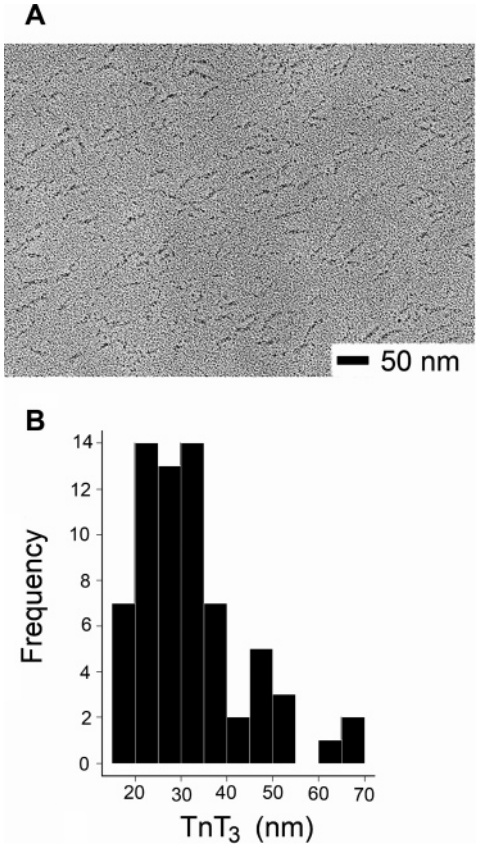

FIGURE 5: Transmission electron microscopy results. (A) Micrograph of shadowed $cTnT_3$ at a magnification of 50000×. (B) Histogram of molecule length measurements.

that the protein, under the conditions we used, was quite homogeneous, suggesting that very little dissociation of the tetramer occurred under the conditions we used.

We have found only one published study that provides evidence for cTnT tetramer formation in solution (*35*). Using size exclusion chromatography and analytical ultracentrifugation, Byers et al. (*35*) showed that cTnT purified from bovine heart exists as a tetramer and suggested a monomer−tetramer self-association model with an equilibrium constant of 6×10^3 mL^3/mg^3. This corresponds to a monomer−tetramer dissociation constant of 2 μmol/L, according to the formulas reported by Bujalowski and Lohman (*37*) and the molecular weight calculated from the primary sequence of the major adult bovine cTnT (*38*).

For the the purposes of comparison, we analyzed our data using a dimer−tetramer reversible self-association model (see Table 1). The molecular weight of the dimer estimated from this model was close to the expected molecular weight of a cTnT dimer. Therefore, our data suggest a dimer−tetramer equilibrium and indicate that the major species of cTnT in solution is a tetramer and the minor component a dimer. If any monomer was present, it was undetectable.

The frictional ratio measured in the velocity experiments is an indicator of the shape of a molecule. The value of f/f_0, estimated from the whole boundary analysis of the velocity data, ranged from 2.16 to 2.35, similar to the value of 2.4 reported previously (*35*, *39*). These ratios are consistent with elongated molecules (globular proteins have f/f_0 values of 1.15−1.30). Modeling the sedimentation velocity data, using an f/f_0 of 2.25 for the tetramer and an oblate ellipsoid model,

predicted a molecule with major and minor diameters of 23.6 and 5.6 nm, respectively. The model of an ideal prolate ellipsoid predicted major and minor diameters of ~60 and 2.2 nm, respectively. These dimensions are consistent with our electron microscopy results.

Our study provides the first direct measurement of the length of cTnT. Byers et al. previously estimated the length of cTnT using an indirect method and derived a Stokes radius of 6.5 nm by extrapolating the relation between Stokes radius and protein concentration to zero. We could not find a report that determined the MW of skeletal TnT in solution to relate it to this Stokes radius or to the length of skeletal TnT, 18.5 ± 3.5 nm estimated by Flicker (*40*) using transmission electron microscopy. Ascribing a precise length to the $cTnT_3$ molecule is difficult because of the large variability of the observed lengths. On the basis of cTnT forming tightly associated stable tetramers, we hypothesize that the most frequently represented molecule in the length distribution (20−40 nm) corresponds to the tetramer.

Summary. Biochemical and biophysical studies of cTnT must be designed and interpreted in a manner that recognizes cTnT self-associates strongly in solution.

REFERENCES

1. Tobacman, L. S. (1996) Thin filament-mediated regulation of cardiac contraction, *Annu. Rev. Physiol. 58*, 447−481.
2. Chandra, M., Montgomery, D. E., Kim, J. J., and Solaro, R. J. (1999) The N-terminal region of troponin T is essential for the maximal activation of rat cardiac myofilaments, *J. Mol. Cell. Cardiol. 31*, 867−880.
3. Gomes, A. V., Guzman, G., Zhao, J., and Potter, J. D. (2002) Cardiac troponin T isoforms affect the Ca^{2+} sensitivity and inhibition of force development. Insights into the role of troponin T isoforms in the heart, *J. Biol. Chem. 277*, 35341−35349.
4. Gomes, A. V., Venkatraman, G., Davis, J. P., Tikunova, S. B., Engel, P., Solaro, R. J., and Potter, J. D. (2004) Cardiac troponin T isoforms affect the Ca^{2+} sensitivity of force development in the presence of slow skeletal troponin I: Insights into the role of troponin T isoforms in the fetal heart, *J. Biol. Chem. 279*, 49579−49587.
5. Morimoto, S., Lu, Q. W., Harada, K., Takahashi-Yanaga, F., Minakami, R., Ohta, M., Sasaguri, T., and Ohtsuki, I. (2002) Ca^{2+}-desensitizing effect of a deletion mutation ΔK210 in cardiac troponin T that causes familial dilated cardiomyopathy, *Proc. Natl. Acad. Sci. U.S.A. 99*, 913−918.
6. Morimoto, S., Yanaga, F., Minakami, R., and Ohtsuki, I. (1998) Ca^{2+}-sensitizing effects of the mutations at Ile-79 and Arg-92 of troponin T in hypertrophic cardiomyopathy, *Am. J. Physiol. 275*, C200−C207.
7. Rust, E. M., Albayya, F. P., and Metzger, J. M. (1999) Identification of a contractile deficit in adult cardiac myocytes expressing hypertrophic cardiomyopathy-associated mutant troponin T proteins, *J. Clin. Invest. 103*, 1459−1467.
8. Szczesna, D., Zhang, R., Zhao, J., Jones, M., Guzman, G., and Potter, J. D. (2000) Altered regulation of cardiac muscle contraction by troponin T mutations that cause familial hypertrophic cardiomyopathy, *J. Biol. Chem. 275*, 624−630.
9. Venkatraman, G., Gomes, A. V., Kerrick, W. G., and Potter, J. D. (2005) Characterization of troponin T dilated cardiomyopathy mutations in the fetal troponin isoform, *J. Biol. Chem. 280*, 17584−17592.
10. Wu, A. H., Feng, Y. J., Moore, R., Apple, F. S., McPherson, P. H., Buechler, K. F., and Bodor, G. (1998) Characterization of cardiac troponin subunit release into serum after acute myocardial infarction and comparison of assays for troponin T and I. American Association for Clinical Chemistry Subcommittee on cTnI Standardization, *Clin. Chem. 44*, 1198−1208.
11. Fahie-Wilson, M. N., Carmichael, D. J., Delaney, M. P., Stevens, P. E., Hall, E. M., and Lamb, E. J. (2006) Cardiac troponin T circulates in the free, intact form in patients with kidney failure, *Clin. Chem. 52*, 414−420.
12. Martin, A. F. (1981) Turnover of cardiac troponin subunits. Kinetic evidence for a precursor pool of troponin-I, *J. Biol. Chem. 256*, 964−968.
13. Tsukui, R., and Ebashi, S. (1973) Cardiac troponin, *J. Biochem. 73*, 1119−1121.
14. Anderson, P. A., and Oakeley, A. E. (1989) Immunological identification of five troponin T isoforms reveals an elaborate maturational troponin T profile in rabbit myocardium, *Circ. Res. 65*, 1087−1093.
15. McMahon, D. K., Anderson, P. A., Nassar, R., Bunting, J. B., Saba, Z., Oakeley, A. E., and Malouf, N. N. (1994) C2C12 cells: Biophysical, biochemical, and immunocytochemical properties, *Am. J. Physiol. 266*, C1795−C1802.
16. Laue, T. M., Shah, B. D., Ridgeway, T. M., and Pelletier, S. L. (1992) Computer-aided interpretation of analytical sedimentation data of proteins, in *Analytical Ultracentrifugation in Biochemistry and Polymer Science* (Harding, S. E., Rowe, A. J., and Horton, J. C., Eds.) pp 90−125, Royal Society of Chemistry, Cambridge, U.K.
17. Durchschlag, H. (1986) Specific volumes of biological macromolecules and some other molecules of biological interest, in *Thermodynamic Data for Biochemistry and Biotechnology* (Hinz, H.-J., Ed.) pp 45−128, Springer-Verlag, Berlin.
18. Demeler, B. (2005) UltraScan: A Comprehensive Data Analysis Software Package for Analytical Ultracentrifugation Experiments, in *Modern Analytical Ultracentrifugation: Techniques and Methods* (Scott, D. J., Harding, S. E., and Rowe, A. J., Eds.) pp 210−229, Royal Society of Chemistry, Cambridge, U.K.
19. Demeler, B., and van Holde, K. E. (2004) Sedimentation velocity analysis of highly heterogeneous systems, *Anal. Biochem. 335*, 279−288.
20. Cao, W., and Demeler, B. (2005) Modeling analytical ultracentrifugation experiments with an adaptive space-time finite element solution of the Lamm equation, *Biophys. J. 89*, 1589−1602.
21. Demeler, B., and Saber, H. (1998) Determination of molecular parameters by fitting sedimentation data to finite-element solutions of the Lamm equation, *Biophys. J. 74*, 444−454.
22. Erickson, H. P. (1995) FtsZ, a prokaryotic homolog of tubulin, *Cell 80*, 367−370.
23. Fowler, W. E., and Erickson, H. P. (1979) Trinodular structure of fibrinogen. Confirmation by both shadowing and negative stain electron microscopy, *J. Mol. Biol. 134*, 241−249.
24. Ricchiuti, V., Voss, E. M., Ney, A., Odland, M., Anderson, P. A., and Apple, F. S. (1998) Cardiac troponin T isoforms expressed in renal diseased skeletal muscle will not cause false-positive results by the second generation cardiac troponin T assay by Boehringer Mannheim, *Clin. Chem. 44*, 1919−1924.
25. Chen, Y., Serfass, R. C., Mackey-Bojack, S. M., Kelly, K. L., Titus, J. L., and Apple, F. S. (2000) Cardiac troponin T alterations in myocardium and serum of rats after stressful, prolonged intense exercise, *J. Appl. Physiol. 88*, 1749−1755.
26. Malouf, N. N., McMahon, D., Oakeley, A. E., and Anderson, P. A. (1992) A cardiac troponin T epitope conserved across phyla, *J. Biol. Chem. 267*, 9269−9274.
27. Ingraham, R. H., and Swenson, C. A. (1984) Binary interactions of troponin subunits, *J. Biol. Chem. 259*, 9544−9548.
28. Johnson, M. L., Correia, J. J., Yphantis, D. A., and Halvorson, H. R. (1981) Analysis of data from the analytical ultracentrifuge by nonlinear least-squares techniques, *Biophys. J. 36*, 575−588.
29. Demeler, B., Saber, H., and Hansen, J. C. (1997) Identification and interpretation of complexity in sedimentation velocity boundaries, *Biophys. J. 72*, 397−407.
30. Takahashi-Yanaga, F., Morimoto, S., Harada, K., Minakami, R., Shiraishi, F., Ohta, M., Lu, Q. W., Sasaguri, T., and Ohtsuki, I. (2001) Functional consequences of the mutations in human cardiac troponin I gene found in familial hypertrophic cardiomyopathy, *J. Mol. Cell. Cardiol. 33*, 2095−2107.
31. Szczesna, D., Zhang, R., Zhao, J., Jones, M., and Potter, J. D. (1999) The role of the NH_2- and COOH-terminal domains of the inhibitory region of troponin I in the regulation of skeletal muscle contraction, *J. Biol. Chem. 274*, 29536−29542.
32. Byers, D. M., McCubbin, W. D., and Kay, C. M. (1979) Hydrodynamic properties of bovine cardiac troponin, *FEBS Lett. 104*, 106−110.
33. Lovell, S. J., and Winzor, D. J. (1977) Self-association of troponin, *Biochem. J. 167*, 131−136.

34. Takeda, S., Yamashita, A., Maeda, K., and Maeda, Y. (2003) Structure of the core domain of human cardiac troponin in the Ca^{2+}-saturated form, *Nature 424*, 35−41.
35. Byers, D. M., and Kay, C. M. (1983) Hydrodynamic properties of bovine cardiac troponin-I and troponin-T, *J. Biol. Chem. 258*, 2951−2954.
36. Anderson, P. A., Malouf, N. N., Oakeley, A. E., Pagani, E. D., and Allen, P. D. (1991) Troponin T isoform expression in humans. A comparison among normal and failing adult heart, fetal heart, and adult and fetal skeletal muscle, *Circ. Res. 69*, 1226−1233.
37. Bujalowski, W., and Lohman, T. M. (1991) Monomer-tetramer equilibrium of the *Escherichia coli* ssb-1 mutant single strand binding protein, *J. Biol. Chem. 266*, 1616−1626.
38. Leszyk, J., Dumaswala, R., Potter, J. D., Gusev, N. B., Verin, A. D., Tobacman, L. S., and Collins, J. H. (1987) Bovine cardiac troponin T: Amino acid sequences of the two isoforms, *Biochemistry 26*, 7035−7042.
39. Siegel, L. M., and Monty, K. J. (1966) Determination of molecular weights and frictional ratios of proteins in impure systems by use of gel filtration and density gradient centrifugation. Application to crude preparations of sulfite and hydroxylamine reductases, *Biochim. Biophys. Acta 112*, 346−362.
40. Flicker, P. F., Phillips, G. N., Jr., and Cohen, C. (1982) Troponin and its interactions with tropomyosin. An electron microscope study, *J. Mol. Biol. 162*, 495−501.

BI7012596